

# Integrating Analytical and Numerical Approaches to Quantify Flow Work in Rate-of-Rise Gas Flow Standards

M. K. Low<sup>1\*</sup>, A. N. Johnson<sup>1</sup>, P. Natarajan<sup>2</sup>, J. G. Pope<sup>1</sup>

<sup>1</sup> National Institute of Standards and Technology, 100 Bureau Dr, Gaithersburg, MD 20877, USA

<sup>2</sup> The George Washington University, 2121 I St NW, Washington, DC 20052, USA

\* E-mail: max.low@nist.gov

## Abstract

Flow work makes it challenging to directly measure the gas temperature in rate-of-rise (RoR) standard collection tanks during filling. Also known as the heat of compression, flow work produces a transient, spatially non-uniform temperature profile that probes have difficulty measuring. Knowing the average gas temperature during filling is necessary for the accuracy of mass flow rate calculation in RoR standards, and so overcoming the flow work issue is vital. To address this challenge, the Fluid Metrology Group at the National Institute of Standards and Technology (NIST) has developed an analytic thermal model to infer the gas temperature in the tank during filling rather than measure it directly. This model shows how to minimize the change in gas temperature due to flow work in a cylindrical tank and was used to guide design for constructing NIST's Semiconductor Low Flow Standard (SLOWFlowS). The standard has been experimentally validated to work within the range of 0.01 sccm<sup>1</sup> to 1000 sccm, with expanded uncertainties in flow rates as low as 0.06%.

However, the thermal model relies on many assumptions that do not hold for flow rates outside of the range of 0.01 sccm to 1000 sccm, alternative collection tank geometries, or gases with exotic thermophysical properties. It is impractical for NIST to experimentally test all these edge cases; therefore, we have performed computational fluid dynamics (CFD) to both assess the validity of assumptions in the analytical model and to extend the capability of SLOWFlowS. These validated CFD models provide a physics-based framework for optimizing future RoR standards and quantifying the influence of flow work across a wide range of operating conditions.

## 1. Introduction

### 1.1 Rate-of-rise flow standards

A flow standard is a high-precision system used to calibrate flow meters by determining mass flow rate using either volumetric methods, which determine mass from measured density in a known-volume tank, or gravimetric methods, which directly measure collected mass. These standards may operate dynamically using time-resolved accumulation data or statically using the net mass or volume accumulated over a defined time interval [1].

Rate-of-rise flow standards are dynamic volumetric standards commonly used for gas flow measurements. In this method, gas flows into a rigid collection tank of known volume, and the mass flow rate is determined from the temporal increase in gas density within the tank. The gas density is calculated from measured pressure and temperature using an appropriate equation of state. Consequently, the accuracy of the flow determination depends strongly on the accuracy of the pressure and temperature measurements. During tank filling, the calculated density increases approximately linearly with

time. A linear regression is applied to the density-versus-time data, and the slope of this best-fit line is multiplied by the known tank volume to determine the mass flow. This measurement principle is illustrated in **Figure 1**.

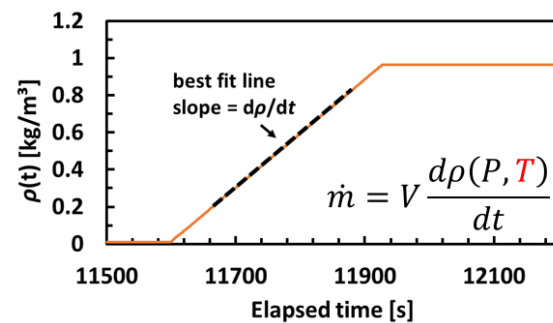


**Figure 1:** Determination of mass flow in a rate-of-rise flow standard. The mass flow is obtained from the slope of the density-versus-time data during tank filling, multiplied by the known collection volume.

Gas pressure during tank filling can be easily measured with high temporal resolution using fast-response pressure transducers; however, accurate measurement of the gas temperature presents a significantly greater

<sup>1</sup> The unit sccm is standard cubic centimeters per minute where the standard volumetric flow  $\dot{V}_{std}$  is obtained by dividing the mass flow rate  $\dot{m}$  by the reference gas density, assuming ideal-gas behavior at the standard conditions  $T_{std} = 273.15$  K and  $P_{std} = 101.325$  kPa.

challenge. Compression heating associated with flow work during filling produces a transient and spatially non-uniform temperature field within the collection tank, which is difficult to characterize using intrusive temperature probes. Additional limitations, including sensor response time and the risk of probe fouling or flow disturbance, further obstruct direct measurement of the gas temperature. As a result, obtaining an accurate temperature for use in density calculations represents a primary source of uncertainty in rate-of-rise flow standards.

To address this challenge, the Fluid Metrology Group at the National Institute of Standards and Technology (NIST) has developed an analytic thermal model [2] that enables the gas temperature during filling to be inferred rather than measured directly. The model provides quantitative insight into the effects of flow work and heat transfer and has been used to guide the design of the NIST Semiconductor Low Flow Standard (SLOWFlowS), with the objective of minimizing temperature non-uniformities within the collection volume.

### 1.2 Thermal Model

The analytic thermal model developed by Johnson et al. informs the design of the collection tank by minimizing flow work effects, thereby simplifying the determination of gas temperature for density calculations. This model relies on assumptions that hold only for collection tanks of high aspect ratio (length over diameter), and in doing so relates the volume-averaged temperature rise due to flow work,  $\Delta T$ , to the collection tank wall temperature,  $T_w$ , through the thermal response factor  $\varepsilon$ :

$$\frac{\Delta T}{T_w} = \frac{\varepsilon}{1 - \varepsilon} \quad (1)$$

The thermal response factor quantifies the relative importance of compressive heating from flow work compared to radial heat conduction to the tank walls and governs the deviation of the gas temperature from  $T_w$  during filling. It is given by

$$\varepsilon = \frac{\dot{m} N_R R_g}{8\pi k L} = \frac{\dot{V}_{std} N_R P_{std}}{8\pi k L T_{std}} \quad (2)$$

where  $\dot{m}$  is the fluid's mass flow,  $N_R$  accounts for real gas effects such as compressibility,  $R_g$  is the specific gas constant,  $k$  is the gas thermal conductivity, and  $L$  is the collection tank length. The expression may be written equivalently in terms of the volumetric flow rate at standard conditions  $\dot{V}_{std}$ , with  $P_{std}$  and  $T_{std}$  denoting the pressure and temperature at standard conditions and assuming ideal gas in that case. Equation (1) shows that reducing the thermal response factor directly reduces the temperature rise due to flow work. This can be achieved by increasing the collection tank length, which increases the available surface area for radial heat conduction; operating at lower flow rates, which reduces compressive heating; and selecting gases with higher thermal

conductivity, which more rapidly dissipates heat to the tank walls.

While this thermal model has proven effective for the current implementation of SLOWFlowS, it relies on simplifying assumptions that limit its applicability to more general flow standard configurations. For alternate collection tank geometries, extended flow ranges, or gases exhibiting significant species-dependent or non-ideal behavior, the model may no longer accurately describe the thermal response and cannot be relied upon to correctly estimate flow work effects. To address these limitations, the Fluid Metrology Group has implemented a computational fluid dynamics (CFD) model based on the full Navier–Stokes equations, enabling analysis of more general flow standard configurations without reliance on the simplifying assumptions of the analytic thermal model. A two-dimensional axisymmetric model has been implemented and validated against experimental measurements, demonstrating good agreement under the operating conditions studied. In parallel, a three-dimensional model that fully captures convective effects is under refinement to extend the analysis to more complex geometries and flow regimes.

## 2. Numerical Setup

### 2.1 Geometry and Meshing

To simulate flow work effects in NIST's SLOWFlowS, computational studies were performed using COMSOL Multiphysics<sup>2</sup> using two-dimensional and three-dimensional cylindrical models with dimensions matching the SLOWFlowS collection tank tubing. The collection tank consists of two redundant volumes: a smaller tank composed of two lengths of stainless-steel tubing, and a larger tank composed of sixteen tubing lengths that incorporates the smaller tank. In this work, only the smaller tank was modeled. Scaling laws inherent to the standard's design allow results obtained for the smaller tank to be used to predict the thermal behavior of the larger collection volume.

The smaller collection tank was modeled as a hollow, dead-end cylinder with an inner diameter of 1.27 cm and a length of 366 cm. The tube wall thickness was 0.254 cm. This geometry was selected based on thermal models which demonstrate that large ( $> 160$ ) aspect ratios minimize flow work effects by promoting radial heat conduction to the tank walls.

#### 2.1.1 2D Model

The two-dimensional model represents an axisymmetric section of the SLOWFlowS collection tank with the same length, inner radius, and wall thickness as the physical tubing described in Section 2.1. The model consists of a longitudinal half-plane with rotational symmetry about the tank centerline. This axisymmetric formulation assumes negligible azimuthal variation and captures the dominant radial and axial heat transfer mechanisms.

<sup>2</sup> Certain commercial equipment, instruments, or materials (or suppliers, or software, ...) are identified in this paper to foster understanding. Such identification does not imply recommendation or endorsement by the National Institute of

Standards and Technology, nor does it imply that the materials or equipment identified are necessarily the best available for the purpose.

The mesh employs spatially varying element sizes to provide increased resolution near the tube wall and gas–solid interface, where the largest temperature gradients occur. Coarser elements are used toward the centerline to reduce computational cost. The final 2D mesh consisted of ~330000 elements. A representative section of the 2D geometry and mesh is shown in **Figure 2**.

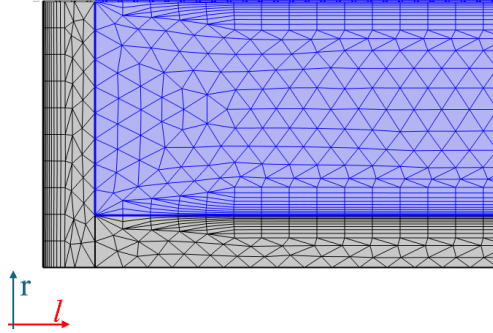


**Figure 2.** Magnified view of the dead-end section of the 2D axisymmetric model showing radially varying mesh refinement used to resolve heat transfer at the fluid–wall interface. The fluid domain is highlighted in blue, while the surrounding unhighlighted region represents the stainless-steel tube wall. Only one half of the cross-section is modeled; axisymmetry about the axial centerline is applied during simulation.

### 2.1.2 3D Model

The three-dimensional model uses the same geometric dimensions as the 2D axisymmetric model but resolves the full circumferential domain, allowing azimuthal variations and convective structures to be captured. Both the fluid and stainless-steel solid domains are explicitly modeled.

To balance accuracy and computational efficiency, the internal fluid domain was divided into three concentric regions with progressively coarser mesh resolution toward the centerline. The finest mesh was applied adjacent to the tube wall to resolve thermal boundary layers and near-wall flow features. The final 3D mesh consisted of  $\sim 2 \times 10^6$  domain elements,  $\sim 300,000$  boundary elements, and  $\sim 20,000$  edge elements.

A representative inlet section of the 3D geometry and mesh is shown in **Figure 3**.

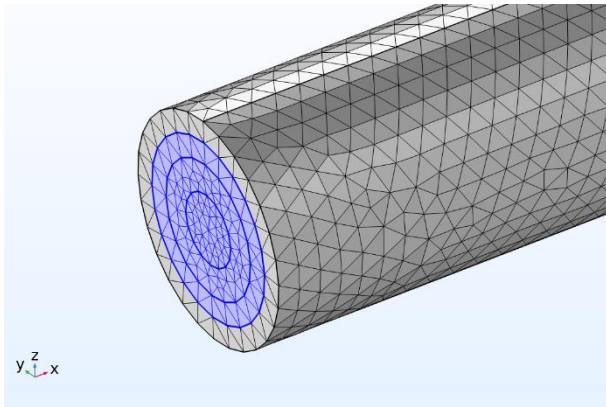


**Figure 3.** Magnified inlet section of the 3D model, with radially varying mesh fineness for computational speed. The fluid domains are highlighted in blue; the stainless-steel domains are unhighlighted.

## 2.2 Mathematical Model

To capture gas heating due to flow work and subsequent heat transfer through the collection tank walls, a coupled fluid flow and heat transfer model [3] was implemented using the governing equations for compressible, low Mach number flow. Gas flow into the tank was treated as compressible with a Mach number  $Ma < 0.3$ , such that density variations due to pressure and temperature changes were retained while acoustic effects were neglected.

### 2.2.1 Mass Conservation

Mass conservation in the collection tank is enforced through the compressible continuity equation,

$$\frac{\partial \rho}{\partial t} + \nabla \cdot (\rho \mathbf{u}) = 0 \quad (3)$$

where  $\rho$  is the fluid's density and  $\mathbf{u}$  is the velocity vector of the fluid. This allows for mass accumulation within the closed volume during tank filling. Density is treated as a function of pressure and temperature through an appropriate equation of state, providing coupling between the continuity, momentum, and energy equations.

### 2.2.2 Momentum Conservation

Momentum conservation is described by the compressible Navier–Stokes equations,

$$\rho \left( \frac{\partial \mathbf{u}}{\partial t} + \mathbf{u} \cdot \nabla \mathbf{u} \right) = -\nabla P + \nabla \cdot \boldsymbol{\tau} + \rho \mathbf{g} \quad (4)$$

where  $P$  is the static pressure,  $\mathbf{g}$  is the acceleration due to gravity, and  $\boldsymbol{\tau}$  is the viscous stress tensor. Viscous effects are retained to accurately capture near-wall flow behavior and its contribution to thermal transport.

### 2.2.3 Energy Conservation

Heat transfer in the fluid and solid domains is described by the energy equation,

$$\rho C_v \frac{\partial T}{\partial t} + \rho C_p \mathbf{u} \cdot \nabla T + P(\nabla \cdot \mathbf{u}) + \nabla \cdot \mathbf{q} = Q + \Phi \quad (5)$$

where,  $C_p$  is specific heat at constant pressure,  $T$  is temperature,  $Q$  is the volumetric heat source due to flow work, and  $\Phi$  is the dissipation function.  $q$  is the conductive heat flux, which is given as the typical Fourier's law  $q = -k\nabla T$ .

## 2.3 Boundary and Initial Conditions

At the inlet, gas enters the collection tank at a prescribed mass flow rate corresponding to the experimental operating conditions. The inlet gas temperature was fixed at  $T_w = 297.15$  K, and the inlet pressure was not prescribed and evolved naturally due to mass accumulation within the closed tank. Flow was assumed to be laminar due to the low-speed flow and narrow pipe dimensions. The downstream end of the collection tank was modeled as a closed, dead-end boundary with zero velocity, allowing pressure to increase during filling. At all fluid–solid interfaces, no-slip velocity conditions were applied. Heat transfer between the gas and the stainless-steel tank walls was modeled using conjugate heat transfer, enforcing continuity of temperature and heat flux across the interface. Heat conduction within the

tank walls was solved explicitly. The outer surface of the stainless-steel tubing was held at a constant temperature equal to the surrounding bath temperature, representing the thermostatically controlled environment of the collection tank. Initial conditions of the tank consisted of uniform pressure  $P = 19.7$  kPa and temperature  $T_w$  throughout the fluid and solid domains, corresponding to the initial tank pressure and bath temperature, respectively, with zero initial velocity. For the two-dimensional model, an axisymmetric boundary condition was applied along the tank centerline.

### 3. Results

#### 3.1 2D Comparisons to Thermal Model

A series of simulations was performed to assess the assumptions underlying the analytical thermal model and to evaluate its applicability across flow rates and gas species. Two sets of cases were considered. In the first set, nitrogen was simulated at four flow rates (75 sccm, 100 sccm, 150 sccm, and 250 sccm) to examine the dependence of flow work heating on flow rate. In the second set, four different gases were simulated at a fixed flow rate of 100 sccm to investigate gas species effects on flow work induced heating. To quantify heating due to flow work, the difference between the volume-averaged gas temperature and the collection tank wall temperature was computed and is reported as  $\Delta T$ . The wall temperature was equal to the initial gas temperature. All simulations were run for 133 s to ensure that thermal equilibrium was reached; however, because the transient heating occurs on a much shorter timescale, the figures in this section are limited to the first 2 s for clarity.

##### 3.1.1 Gas Species Effects at 100 sccm

Figure 4 shows the temporal evolution of  $\Delta T$  for four gases flowing at 100 sccm. The results demonstrate that the design guidance provided by the analytical thermal model is effective: the large length-to-diameter ratio of the collection tank promotes rapid radial heat conduction to the walls, resulting in a short ( $< 1$  s) thermal transient and a small deviation ( $< 0.4$  K) of the gas temperature from the wall temperature. This behavior reduces the sensitivity of the density calculation to transient gas heating in SLowFlowS.

Differences in the magnitude and relaxation time of  $\Delta T$  among the gases are primarily attributable to variations in various thermophysical properties such as thermal conductivity and volumetric heat capacity.

Table 1 contains values for the temperature rise measured experimentally on SLowFlowS as well as predictions by the analytical thermal model and the corresponding CFD results. The difference in results is discussed in a later section.

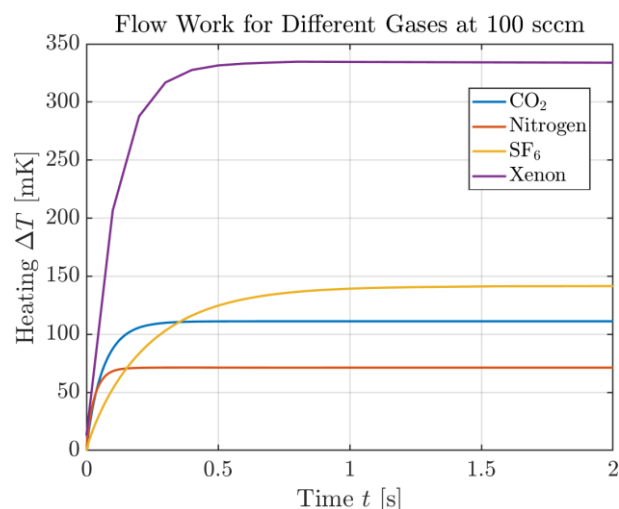


Figure 4. CFD results for volume-averaged gas temperature rise due to flow work,  $\Delta T$ , for four gases flowing into the collection tank at a nominal flow rate of 100 sccm. The wall temperature is held fixed and used as the reference temperature. All cases exhibit a rapid transient followed by an asymptotic approach to thermal equilibrium, with the steady-state temperature rise depending on gas thermophysical properties.

Table 1. Comparison of steady-state flow work heating predicted by the analytical model and by CFD simulations for different gases at 100 sccm. Values correspond to the asymptotic volume-averaged gas temperature rise relative to the wall temperature. For xenon, the uncertainty interval exceeds the plotting scale due to instrumentation factors and is therefore not displayed; this does not alter the qualitative agreement among the three approaches.

Gas	Experimental [mK]	Exp. Uncertainty (k=2) [%]	CFD [mK]	Model [mK]
CO <sub>2</sub>	151	16	117.7	121.9
Nitrogen	68	43	73.8	77.7
SF <sub>6</sub>	180	35	141.6	157.9
Xenon	383	-	330.2	364.3

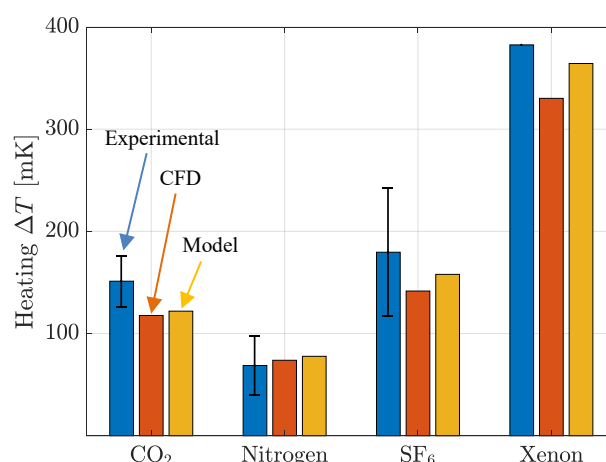
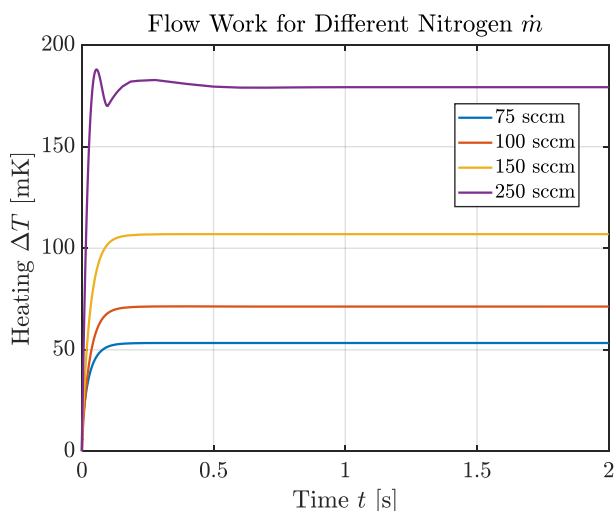


Figure 5. Visualization of Table 1 data.

##### 3.1.1 Flow Rate Effects with Nitrogen

Figure 5 shows the evolution of  $\Delta T$  for nitrogen at flow rates of 75 sccm, 100 sccm, 150 sccm, 250 sccm. As in the gas species study, the temperature rise due to flow work occurs on a short ( $< 0.1$  s) timescale and asymptotes

rapidly as heat is conducted to the tank walls. Increasing flow rate results in a larger transient temperature rise, consistent with increased compressive heating. Quantitative differences between the analytical thermal model and the CFD results for each flow rate, as well as the experimentally determined values, are summarized in **Table 2**. While the overall trends are consistent between the two modeling approaches, systematic deviations are observed, motivating further analysis of the underlying model assumptions.



**Figure 6.** CFD results for volume-averaged gas temperature rise due to flow work for nitrogen at different flow rates. At the highest flow rate 250 sccm, a brief temperature overshoot is observed prior to equilibration, possibly reflecting enhanced convective transport during the initial filling transient.

**Table 2.** Comparison of steady-state flow work for different flow rates of nitrogen. Values correspond to the asymptotic volume-averaged gas temperature rise relative to the wall temperature. Experimental data for 250 sccm was not taken due to limitations of the standard and is omitted. Good agreement is observed within all three values.

Flow [sccm]	Experimental [mK]	Exp. Uncertainty ( $k=2$ ) [%]	CFD [mK]	Model [mK]
75	63	12	54.7	58.2
100	69	42	73.8	77.7
150	104	11	106.9	116.5
250	-	-	179.3	194.3

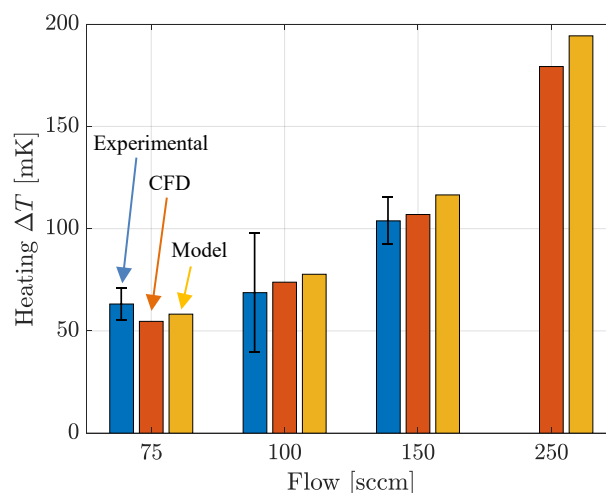


**Figure 7.** Visualization of Table 2 data.

### 3.2 3D Comparisons to Thermal Model

A single three-dimensional simulation was performed to assess whether extending the CFD model from a 2D axisymmetric formulation to a full 3D geometry introduces additional flow work heating not captured in the 2D model. The simulation was conducted for nitrogen at a flow rate of 100 sccm, corresponding to a representative operating condition used in the 2D analysis. For this case, the difference in volume-averaged gas temperature rise,  $\Delta T$ , between the 2D and 3D simulations was less than 7 mK and within numerical uncertainty. As a result, the 3D result is not reported separately in tabular form. This outcome indicates that, under the present geometry and operating conditions, three-dimensional effects such as azimuthal asymmetries and convective motion do not significantly alter the predicted flow work heating relative to the 2D axisymmetric model for nitrogen. This baseline agreement provides a reference point for future investigations of gases or conditions for which three-dimensional convective effects may be more significant.

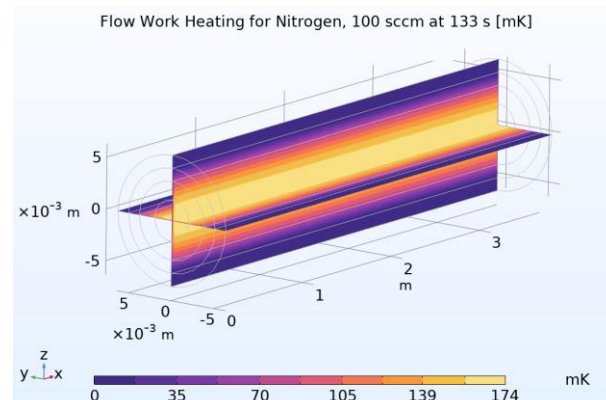


**Figure 8.** Volume-rendered  $\Delta T$  field in the 3D model at  $t = 133$  s for 100 sccm. This visualization is included to illustrate the current three-dimensional implementation and to provide a qualitative assessment of spatial temperature variations, including the absence of pronounced convective structures under the simulated operating conditions.

## 4. Discussion

The results presented in the previous section indicate that the CFD simulations reproduce the qualitative trends predicted by the analytical thermal model, including the rapid transient increase in gas temperature followed by an asymptotic approach toward thermal equilibrium governed by heat transfer to the collection tank walls. Note that in Johnson et al. the transient times are much larger due to the different starting conditions of the flow into the tank in that case; at equal initial conditions the transient times have good agreement. Agreement is also observed in the relative dependence on gas species and flow rate; however, quantitative differences in the predicted steady-state flow work heating remain.

These differences are observed across all simulated conditions and are not unexpected, given that the analytical thermal model has been experimentally validated and was developed to capture the dominant physics governing flow work heating in the SLOWFlowS collection tank, whereas the CFD model represents a numerical approximation of the same physical processes. The thermal model therefore serves as the reference framework for assessing the CFD results, and discrepancies are interpreted as limitations or approximations within the CFD formulation rather than uncertainty in the underlying thermal behavior.

One likely contributor to the observed differences is the treatment of heat transfer within the fluid domain in the CFD simulations. The analytical thermal model assumes heat transfer is dominated by radial conduction to the tank walls, an assumption that has been supported by experimental measurements for the high aspect ratio geometries employed in SLOWFlowS. In contrast, the CFD model permits the development of weak convective motion during the filling transient, even in geometries intended to suppress convection. The presence of such numerically resolved convection may enhance heat transfer to the walls and result in lower volume-averaged gas temperatures than predicted by the validated thermal model. Gas property modeling in the CFD framework may also contribute to the discrepancies, particularly for gases with low thermal conductivity or significant non-ideal behavior. In the present simulations, COMSOL Multiphysics treats all gases as ideal, whereas the thermal model incorporates experimentally informed corrections through real-gas parameters. Differences in effective heat capacity, compressibility, and viscous dissipation under transient conditions may therefore lead to systematic under- or over-prediction of flow work heating in the CFD results for certain gases. Numerical considerations may further influence the CFD predictions, especially at low flow rates where velocity magnitudes are small and viscous dissipation is sensitive to mesh resolution and numerical diffusion. Although mesh refinement was applied near the tube wall to resolve steep thermal gradients, residual numerical effects within the core flow cannot be fully excluded. The consistent qualitative trends observed across flow conditions and the agreement between the 2D and 3D simulations suggest that these numerical effects are secondary, but additional mesh sensitivity and solver studies would be required to fully quantify their contribution.

## 5. Conclusion

The comparison of CFD simulations, experimental measurements, and the analytical thermal model demonstrates consistent trends in flow work heating across gases and flow conditions. Transient simulations indicate steady state conditions occur on the order of  $\leq 1$  s, reducing the uncertainty in the determination of the average gas temperature. Agreement between the CFD and analytical model is within 5 % to 10 % and is within experimental uncertainty, indicating good agreement between the two models despite slight discrepancies.

These observed discrepancies between the CFD simulations and the thermal model do not affect the conclusions regarding the effectiveness of the collection tank design in minimizing flow work heating. The experimentally validated thermal model continues to provide reliable and conservative guidance for standard design and density determination in SLOWFlowS. The CFD simulations are best viewed as a complementary analysis tool, useful for examining departures from the simplifying assumptions of the thermal model and for identifying conditions under which additional physical effects or numerical sensitivities may become relevant. Ongoing refinement of the CFD framework is therefore focused on improving consistency with the validated thermal model and extending its applicability to operating regimes and geometries for which the analytical model may not be directly applicable. In this role, CFD provides a means to explore design variations and parameter spaces that are difficult to access experimentally, supporting future development of flow standards beyond the current SLOWFlowS configuration.

## 6. References

- [1] J. D. Wright, S. Nakao, A. N. Johnson, M. R. Moldover, "Gas flow standards and their uncertainty," *Metrologia*, vol. 60, no. 1, Art. no. 015002, Dec. 2022
- [2] A. N. Johnson, P. Natarajan, J. G. Pope, J. D. Wright, C. J. Crowley, and S. Nakao, "A Non-Intrusive Analytic Temperature Model for Rate-of-Rise-Based Gas Flow Standards", in *Proceedings of the 20<sup>th</sup> International Flow Measurement Conference*, 2026.
- [3] COMSOL AB. *COMSOL Multiphysics® v6.3*. COMSOL AB, Stockholm, Sweden, 2024. Finite element analysis software